Production and Functionalization of cobalt nanofoams for energy storage

Naureen Khanam

naureen.khanam@tecnico.ulisboa.pt

Instituto Superior Técnico, Universidade de Lisboa, Portugal

October 2019

***Abstract*-**Highly porous surface areas with high capacitive and good conductive response are important requirements for materials to be used as supercapacitor electrodes. Metallic cobalt has the advantage of high conductivity and cobalt oxides possess high capacitive response. Cobalt nanofoam was produced on stainless steel substrate by dynamic hydrogen bubble template (DHBT) method to have honeycomb like morphology with cauliflower like agglomerates. Cyclic voltammograms and galvanostatic discharge curves of Co nanofoam indicated a combination of pseudocapacitive and intercalation type response with partial redox wave like features. Nanofoams were treated thermally and chemically for obtaining cobalt oxides with good electrochemical response. Chemically oxidized Co nanofoam with 5% H_2O_2 for 24 hours exhibited specific capacity of 26.1 mAh g^{-1} at 1 Ag^{-1}. An asymmetric cell fabricated with chemically treated Co nanofoam (5% H_2O_2-24h) as positive electrode and carbon as negative electrode, showed pseudocapacitive response with 34.6 Fg^{-1} specific capacitance at 0.1 Ag^{-1}. The highest specific energy was found to be 7.8 Wh kg^{-1} at a power density of 63.6 kW kg^{-1} which did not show any meaningful decrease at 1288 kW kg^{-1}. The cycling stability of the cell was measured with 2000 cycles of galvanostatic charge discharge and only 10% capacitance loss was observed.

***Keywords*-** Co nanofoam, cobalt oxides, DHBT electrodeposition, asymmetric supercapacitor, energy storage

I. INTRODUCTION

Supercapacitors are being investigated as energy storage system due to their excellent cycle life and ability to manage high power rates compared to rechargeable batteries[12]. Efficiency of a supercapacitor largely depends on the performance of the electrode materials and good electrode-electrolyte interaction. High surface area, well-balanced porosity and nanostructure of the active material can help achieving high capacitance and longer stability of the electrode material[3]. Different metal oxides have been used as supercapacitor electrode material because of their high specific capacitance and good conductivity[1]. Among them cobalt oxides are of great interest given their high theoretical capacitance, high reversibility, large surface area as well as high conductivity[4].

3D metallic foams have been of interest in the recent past because of their low cost, easy fabrication, high porosity, high electrical conductivities and light weight with high surface area[5]. Dynamic hydrogen bubble template (DHBT) method is used for the fabrication of metallic nanofoams, where H_2 bubbles evolve by electrodeposition at high overpotentials. Vigorous hydrogen evolution results in microporous honeycomb like structure with cauliflower or dendrite-like nanostructures[6]. The cauliflower like morphology contributes to high surface area because of its nanofeatures and the honeycomb like morphology contributes to the tailored porous structure necessary for the penetration of electrolyte ions. A study discussed about the effect of electrodeposited manganese oxide on bimetallic Ni-Co nanofoam as a composite electrode for supercapacitor application where DHBT method was applied for developing high surface area and tailored porosity[7]. Low density morphological feature was ensured due to enrichment of the nanofoam with cobalt[7]. 3D cobalt foam can ensure high surface area with high porosity which is an important criterion for supercapacitor electrode materials. The present study refers to the production of Co nanofoam by DHBT method and modification to cobalt oxides to evaluate their electrochemical performance of energy storage.

II. EXPERIMENTAL PROCEDURE

The Co foam was electrodeposited on stainless steel (substrate) from 0.1 M $CoCl_2.6H_2O$ + 2 M NH_4Cl solution in a two-electrode electrochemical cell using Pt as the counter electrode. A current of -2.83 Acm^{-2} was supplied from *Sorensen LH 110* DC to the cell for 30 sec while vigorous bubbles were observed at the working electrode. After deposition, the nanofoams were rinsed with water followed by ethanol and dried with compressed air. Before further treatment, the foams were left at room temperature for at least 24 hours for drying. The weight of the active material was measured by weighting the substrate before and after deposition.

Nanofoams were thermally treated for 3 hours at different temperatures ranging from 100^0C to 400^0C in Memmert oven. After treatment, the weight of the active material was measured.

Chemical treatment of the nanofoam was carried out with H_2O_2 of different concentrations from 5%

to 20% for different time range (1 h - 24 h). Optimum concentration and time were selected calculating specific capacitance and further measurements were carried out for chemical treatment with the selected optimized condition (5% H_2O_2 - 24h).

The surface morphology of Co nanofoam and treated Co nanofoam was examined by Scanning electron microscopy with JEOL 7001-F SEM instrument operated at 15 keV. Crystal structure of the nanofoam were determined with X-ray diffraction spectroscopy using the Bruker AXS D8 advance instrument with Cu Kα radiation (1.5418 Å). The diffractograms were obtained between 10^0 and 70^0 with a step size of 0.05^0 and a step time of 20 sec.

Electrochemical measurements were carried out in 1 M KOH with a three-electrode system using Pt as the counter electrode and saturated calomel electrode (SCE) as the reference electrode. Cyclic voltammetry, galvanostatic charge discharge, cycling stability of the Co nanofoam and the treated nanofoams were examined. Electrochemical Impedance Spectroscopy (EIS) and self-discharge of the Co nanofoam were measured also.

To assess the potential of the Co nanofoam and chemically treated nanofoam (5% H_2O_2-24h) to be used in electrochemical cell, asymmetric systems were fabricated with carbon as the negative electrode and Co nanofoam (treated or untreated) as the positive electrode. Cyclic voltammetry, galvanostatic charge discharge and cycling stability of the cells were carried out to measure the performance.

III. RESULTS AND DISCUSSION

Results of Co nanofoam

SEM image of the Co nanofoam indicated in Fig. 1(a) shows the honeycomb like morphology with regular and irregular holes of about 15μm-18μm diameter. In the inset, magnified image shows cauliflower nanostructure. The XRD spectrum (Fig. 1(b)) shows two distinctive peaks at 44.5^0 and 50.7^0 corresponding to (111) and (200) planes of face-centred cubic cobalt (ICDD-00-001-1259).

Cyclic voltammograms of Co nanofoam measured in a potential range from -0.6V to 0.4V at different scan rates (20 mVs^{-1} - 200mVs^{-1}) in 1 M KOH (Fig. 1(c)) show a combination of pseudocapacitive and intercalation partial redox type response[8]. With the increase of scan rates, the area under the curve increases indicating diffusion-controlled electron transfer process. Anodic and cathodic waves also appear for fast scan rates responsible for superficial intercalation and increased resistance on the electrode. Galvanostatic charge discharge curves (Fig. 1(d)) at 1 Ag^{-1} for the potential range from -0.6 V to 0.4 V show almost linear response with some fluctuations. The response substantiates voltammograms indicating combined pseudocapacitive and intercalation redox type response. Faradaic efficiency was calculated with (1):

$$\eta = \frac{t_D}{t_C} \times 100\% \qquad (1)$$

Where, η is the coulombic efficiency, t_D is the discharge time and t_C is the charging time. The efficiency found to be 89.9% which shows small faradic losses during the process due to resistance.

Specific capacitance C for different current densities (1 Ag^{-1}- 6 Ag^{-1}) were calculated from the discharge curves in Fig. 1(e) by the following equation and showed in Table 1

$$C = \frac{I\,\Delta t}{m\Delta V} \qquad (2)$$

where, I denotes the current applied to the sample, m is the mass of the active material, Δt is the time and ΔV denotes the total voltage applied. The specific capacitance for Co nanofoam is 20.4 Fg^{-1} at 1 Ag^{-1} which exhibits ~36% decrease with a six-fold increase of specific current indicating capacitance value of 7.3 Fg^{-1} at 6 Ag^{-1}.

The Electrochemical Impedance Spectroscopy was tested for Co nanofoam at two different potentials, discharged at -0.35 V and charged at 0.35 V that are shown in Fig. 2. The Bode plots and evolution of real and imaginary capacitance calculated from the experimental data along with the Nyquist plots at discharged and charged states are presented. The Bode plots indicate decrease in resistance and negative increase in phase angle in the same frequency range when the material goes from discharge to charge state. The reason of higher resistance at discharged state can be loss of electrolyte ions on the electrode surface when the material is discharged.

Table 1 Specific capacitance of Co nanofoam at different current densities

Specific current Ag^{-1}	**Specific capacitance** Fg^{-1}
1	20.4
2	15.9
4	12.0
6	7.3

The Nyquist plots of both charge and discharge states clearly show that Co nanofoam is conductive at high potential and more resistive at lower potential. The capacitive behaviour of the Co nanofoam was measured by calculating capacitance dependent on frequency, defined as[9]

$$C(\omega) = C'(\omega) + C''(\omega)$$

where,

$$C'(\omega) = \frac{-Z''(\omega)}{\omega|Z(\omega)|^2}$$

$$C''(\omega) = \frac{Z'(\omega)}{\omega|Z(\omega)|^2}$$

And $Z(\omega) = Z'(\omega) + Z''(\omega)$

where $C'(\omega)$ and $C''(\omega)$ indicate the real and imaginary part of the complex capacitance, respectively and $Z'(\omega)$ and $Z''(\omega)$ are the real and imaginary impedance dependent on the frequency, respectively.

$C'(\omega)$ represents the capacitance of the electrode material and the electrode-electrolyte interaction. For the discharged state at -0.35 V (Fig. 2(c)), at higher frequency the material shows poor capacitance. As the frequency decreases, at around 100 Hz, the capacitance increases significantly and almost linearly. For the charged state at 0.35 V (Fig 2(f)), the response at high frequency is similar to the discharged state. The increase in capacitance occurs when the frequency decreases at about 10 Hz and the increase continues exponentially with the lowering of frequency. The reason behind the high capacitive response at low frequency can be explained as the electrode-electrolyte interaction. At higher frequency, the interaction between the electrolyte and cobalt nanofoam is very weak and only limited to the surface of the nanofoam. But at lower frequency, electrolyte can reach the porous bulk of the nanofoam and more active materials take part in the storage process. $C''(\omega)$ expresses dielectric loss of electrolyte ions due to the rotation or movement of the molecules dependent on frequency. Representation of $C''(\omega)$ is used to calculate the factor of merit which is represented by the dielectric relaxation time, t_0. The relaxation time indicates the minimum time necessary to dissipate all the energy of the electrode with an efficiency higher than 50%. The factor of merit calculated at -0.35 V and 0.35 V are 0.09 sec and 0.75 sec, respectively. So, during discharge, Co nanofoam takes less time to dissipate all the energy than to the charged state.

Effect of Thermal treatment

SEM image of thermally treated Co nanofoams at 100^0C and 400^0C in Fig. 3(a). show no difference when treated at 100^0C compared to the Co nanofoam and a transformation is seen when treated at 400^0C (Fig. 3(b)). An oxide layer may form on the metallic Co when treated at 400^0C, which causes the cauliflower structure look like more aggregated. XRD patterns in Fig. 3(c) show peak at 44.5^0 corresponding to (111) plane of face centred cubic cobalt (ICDD-00-001-1259) for treatment at 100^0C, similar to Co nanofoam, while for treatment at 400^0C (Fig. 3(d)) show peaks at 31.2^0, 36.7^0, 38.6^0, 44.5^0, 55.6^0, 59.4^0 and 65.1^0 representing (220), (311), (222), (400), (422), (511) and (440) planes of face-centred cubic Co_3O_4 (ICDD-00-042-1467), respectively. Three other peaks at 43.5^0, 44.3^0 and 50.5^0 are responsible for the substrate stainless steel.

The voltammograms of thermally treated nanofoams at 50 mVs^{-1} shown in Fig. 3(e) represent, for treatment at lower temperature than 250^0C, similar response is seen like the Co nanofoam.

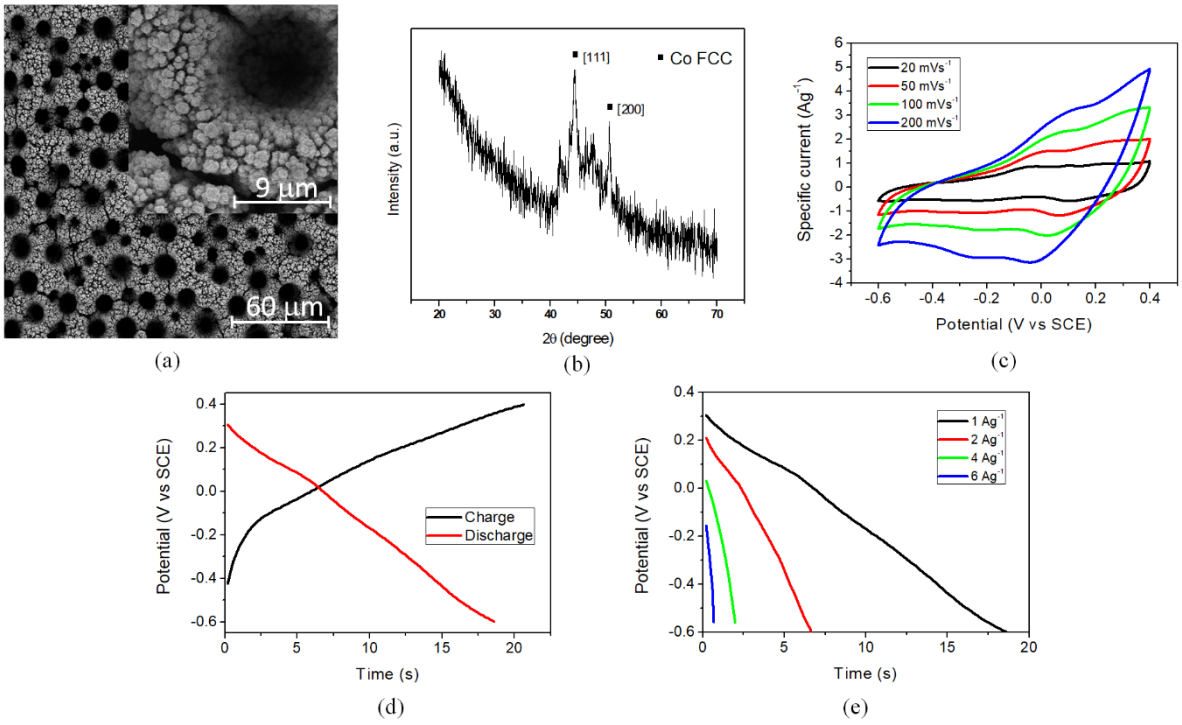

Figure 1 Results of Co nanofoam: SEM image (a); XRD (b); cyclic voltammograms at different scan rates (c); Galvanostatic charge discharge at $1Ag^{-1}$ (d); discharge curves at different current densities (e)

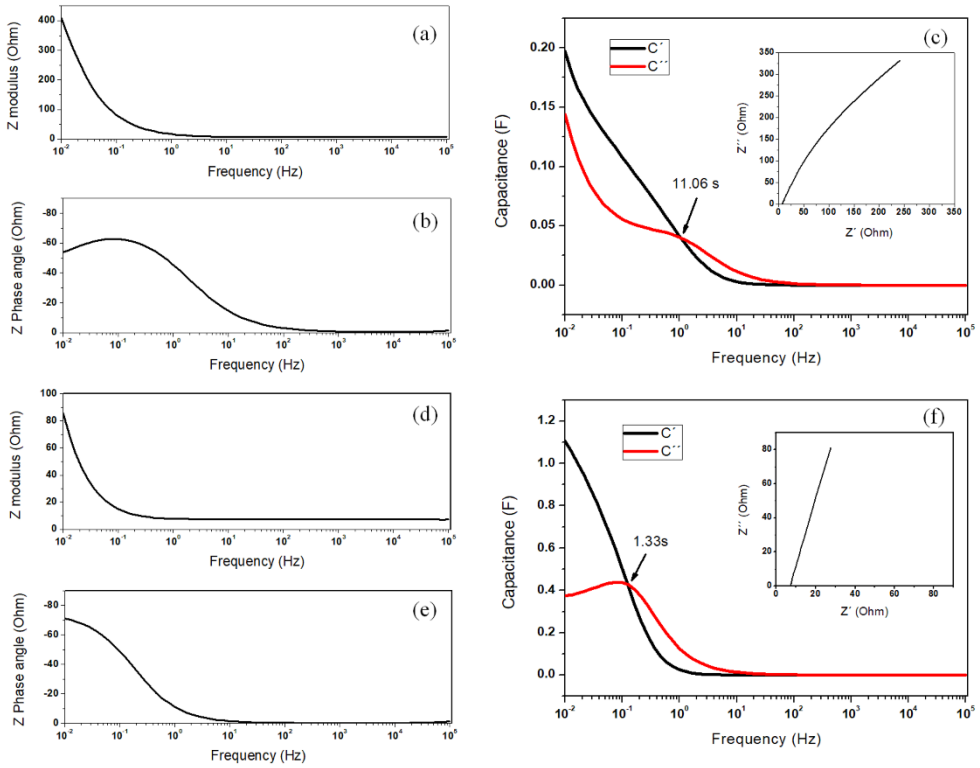

Figure 2 EIS of Co nanofoam: bode plot at -0.35V(a, b); evolution of real and imaginary part of capacitance vs Frequency at -0.35V (c) (Nyquist plot in inset); bode plot at 0.35V(d, e); evolution of real and imaginary part of capacitance vs Frequency at 0.35V (f) (Nyquist plot in inset);

For treatment at higher temperatures than 250^0C, the formation of Co_3O_4 dominates the response that causes decrease of conductivity, as a result smaller area under the voltammogram appears. The more visible redox peaks for nanofoams treated at higher temperatures represent faradaic dominated response and the peaks may be described by the following reactions[10]:

$$Co_3O_4 + OH^- + H_2O \leftrightarrow 3CoOOH + e^-$$

$$CoOOH + OH^- \leftrightarrow CoO_2 + H_2O + e^-$$

Galvanostatic discharge curves in Fig. 3(f) show that, at temperatures higher than 250^0C, more waves appear in the discharge response with a significant decrease in the discharge time compared to lower temperature and to the as produced Co foam (Fig 1(e)) suggesting that the charge storage mechanism is more faradaic dominated. The specific capacitance for nanofoams treated at 100^0C, 200^0C, 250^0C and 400^0C was calculated at $1Ag^{-1}$ and found to be 21.0 Fg^{-1}, 19.0 Fg^{-1}, 6.9 Fg^{-1} and 1.4 Fg^{-1}, respectively. So, the increase of temperature above 250^0C leads to a significant decrease of the capacitance that agrees with the voltammograms as well (Fig. 3(e)).

Effect of chemical treatment

The effect of the concentration of H_2O_2 and treatment times can be explained with Fig. 4 where specific capacitance of the nanofoams with respect to the concentration at 1 Ag^{-1} are demonstrated. The specific capacitances of chemically treated nanofoams (65 Fg^{-1}- 93 Fg^{-1}) are remarkably high compared to the specific capacitance of Co nanofoam (20.4 Fg^{-1}). As the treatment time increases, the specific capacitance increases for the low concentration solution (5% H_2O_2). The specific capacitance of the nanofoam treated with 5% H_2O_2 for 24 hours is calculated to be 95.2 Fg^{-1} which is 42% greater than of the nanofoam treated with 5% H_2O_2 for 1 hour (66.8 Fg^{-1}). For treatment with H_2O_2 of higher concentration (20% in this case), the specific capacitance is almost independent of the treatment time. The nanofoams treated with H_2O_2 of different concentrations for 1 hour show an increase in the capacitance with the increase in the concentration. While for 24 hours treatment time, the increase in the concentration causes decrease in capacitance. Specific capacitance of Co nanofoam treated with 20% H_2O_2 for 24 hours is 73.6 Fg^{-1} which is 22% lower compared to the Co nanofoam treated with 5% H_2O_2 for 24 hours. Comparing all the effects of H_2O_2 concentration and treatment times, treatment with 5% H_2O_2 for 24 hours is considered as the optimized chemical treatment condition.

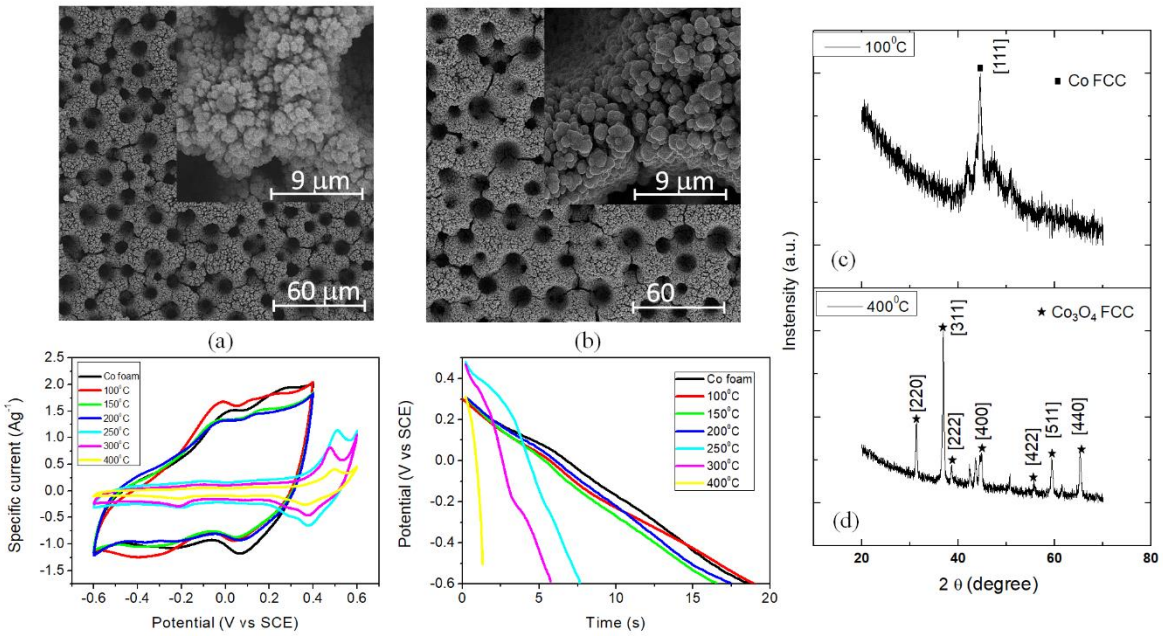

Figure 3 SEM results of thermally treated nanofoam (a) 100^{0}C, (b) 400^{0}C; XRD pattern of thermally treated nanofoam (c) 100^{0}C, (d)400^{0}C; Results of thermal treatment at different temperatures: Voltammograms at 50mVs^{-1}(a); Discharge curves at 1Ag^{-1}

Fig. 5(a) represents the SEM image of chemically treated Co nanofoam with 5% H_2O_2 for 24 hours at two magnifications. The microscopic image illustrates the highly porous honeycomb like morphology, identical to the as produced Co nanofoam. The channels connecting the regular and irregular holes increase in number for the treated nanofoams compared to the untreated Co foam, which accounts for higher surface area and more accessible active sites for the electrolyte ions.

The XRD results in Fig. 5(b) show that the intensity of peak corresponding to (111) plane of face-centred cubic cobalt increases compared to the untreated cobalt foam (Fig. 1(a)), which means that the crystal (111) plane size increases when treated with 5% H_2O_2 for 24 hours. No significant change is visible for (200) plane. No planes of cobalt oxides are seen which probably may because of the poor crystallinity of the phase formed. Therefore, the XRD signals detected are from the bulk of the foam. So, the oxidation due to the chemical treatment is limited to the surface only.

Comparison of the electrochemical response of chemically treated nanofoam (5% H_2O_2 for 24 hours) with the untreated cobalt nanofoam are shown in Fig. 5(c) and Fig. 5(d). The voltammograms (Fig. 5(c)) at 50 mVs^{-1} show a significant increase in the area under the curve for the nanofoam chemically treated in 5% H_2O_2 for 24 hours compared to the cobalt nanofoam. This signifies the remarkable increase of the capacitance due to the treatment. The galvanostatic discharge curves in Fig. 5(d) substantiate the findings of the voltammograms. Specific capacity of the nanofoam at 1 Ag^{-1} indicates an increase of ~360% from 5.7 mAhg^{-1} to 26.1 mAhg^{-1} after treatment.

Cycling stability (Fig. 5(e)) increases from 5% to about 60% after 2000 cycles when the Co nanofoam is chemically treated with 5% H_2O_2 for 24 hours.

Asymmetric cell

A. Carbon testing

Carbon electrodes used for the asymmetric cell were tested electrochemically. The cyclic voltammetry of the carbon material electrode was measured for a range of scan rates (10 mVs^{-1}-100 mVs^{-1}) in the potential range from -0.9 V to 0.2 V. The voltammograms (Fig. 6(a)) evidence a supercapacitive response[8], with increased resistance at higher scan rates. The galvanostatic charge discharge analysis was carried out for 1Ag^{-1} to 10 Ag^{-1} current densities in a potential range from -0.9 V to 0 V. The discharge curves in Fig. 6(b) represent almost a linear response, indicating pseudocapacitive charge storage mechanism. The specific capacitance decreases about 43% from 173 Fg^{-1} to 97 Fg^{-1} for ten-fold increase in current density from 1 Ag^{-1} to 10 Ag^{-1}, respectively.

The capacitance retention was calculated from the discharge curves at 4 Ag^{-1} for 2000 cycles. The excellent capacitance retention (Fig. 6(c)) of carbon indicates high cycling stability due to the better wettability of the carbon surface after soaking in the electrolyte for long time.

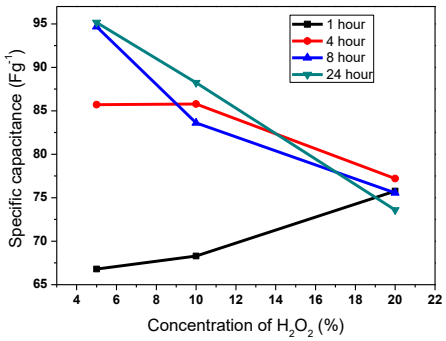

Figure 4 Specific capacitance for chemically treated Co foam at different concentration

B. Co nanofoam - C asymmetric cell

Asymmetric cell was assembled with cobalt nanofoam as the positive electrode and carbon as the negative electrode. Cyclic voltammetry was carried out in 1 M KOH for scan rates from 10 mVs^{-1} to 50 mVs^{-1}. Voltammograms are shown in Fig. 6(d) that indicate a pseudocapacitive response with increased resistance in the potential range above 1.3 V. With the increased scan rate, the capacitance does not change, representing the rate stability of the cell. Galvanostatic discharge curves for current density from 0.1 Ag^{-1} to 1 Ag^{-1} (Fig. 6(e)) exhibit pseudocapacitive response with a capacitance decrease of 50% from 4.5 Fg^{-1} to 2.3 Fg^{-1} calculated at 0.1 Ag^{-1} and 1 Ag^{-1}, respectively.

The capacitance retention plot (Fig. 6(f)) for 2000 cycles indicate rapid capacitance drop for first 100 cycles but good rate stability of the cell afterwards.

C. Co nanofoam (5% H_2O_2 – 24 h) - C asymmetric cell

Chemically treated Co nanofoam with 5% H_2O_2 for 24 hours was used as the positive electrode and carbon as the negative electrode to assemble another asymmetric cell. The cell was studied in 1 M KOH by cyclic voltammetry and galvanostatic charge discharge. The cycling stability was also measured.

The voltammograms in Fig.6(g) measured for different scan rates indicate a pseudocapacitive response of the cell with a combination of intercalation type redox processes. The increase in scan rates show resistive features due to the electrode-electrolyte interaction. Galvanostatic discharge curves in Fig.6(h) for different current densities from 0.1 Ag^{-1} to 2 Ag^{-1} indicate a pseudocapacitive response, showing a decrease in capacitance with current. The specific capacitance for 0.1 Ag^{-1} is 34.6 Fg^{-1} which decreases only 2% to 33.9 Fg^{-1} for 20-fold of increase in current to 2 Ag^{-1} indicating excellent rate stability. The capacitance retention plot (Fig. 6(i)) shows only 10% capacitance lose after 2000 cycles which reveals excellent cycling stability of the asymmetric cell. Specific energy of the cell was calculated as 7.8 Wh kg^{-1} for specific power of 63.6 kW kg^{-1} which did not show any meaningful decrease at 1288 kW kg^{-1}(Fig. 7).

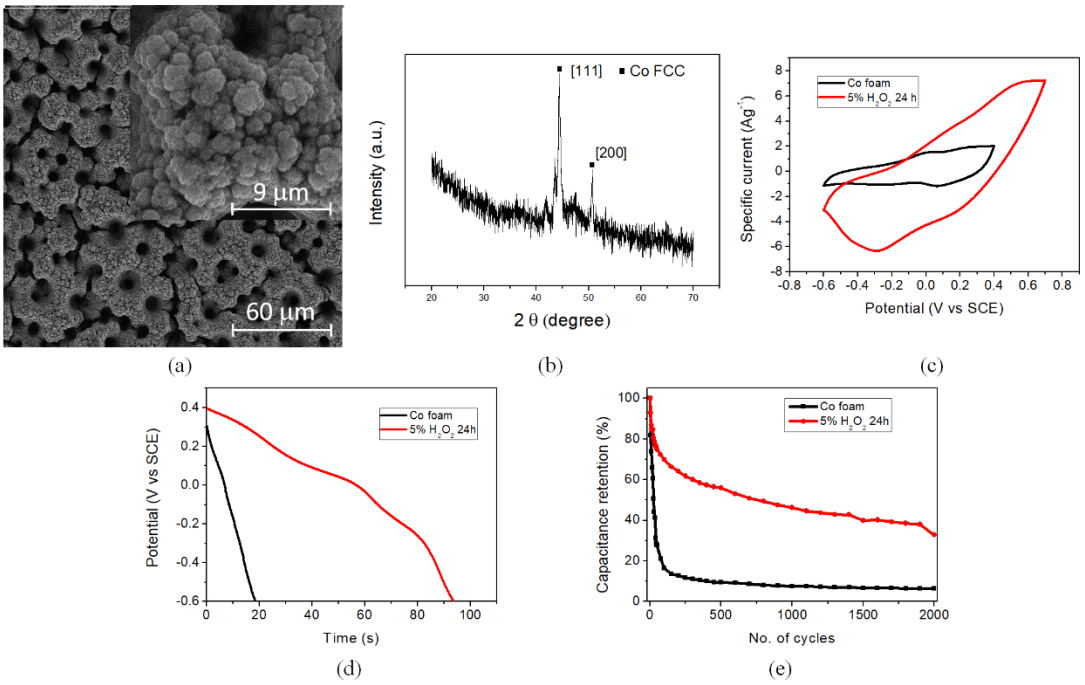

Figure 5 Results of chemically treated nanofoam with 5% H_2O_2 for 24 hours: SEM image (a); XRD patterns (b); Result comparison with cobalt nanofoam: voltammogram at 50 mVs^{-1}(c); Discharge curves at 1Ag^{-1}(d); Cycling stability for 2000 cycles (e)

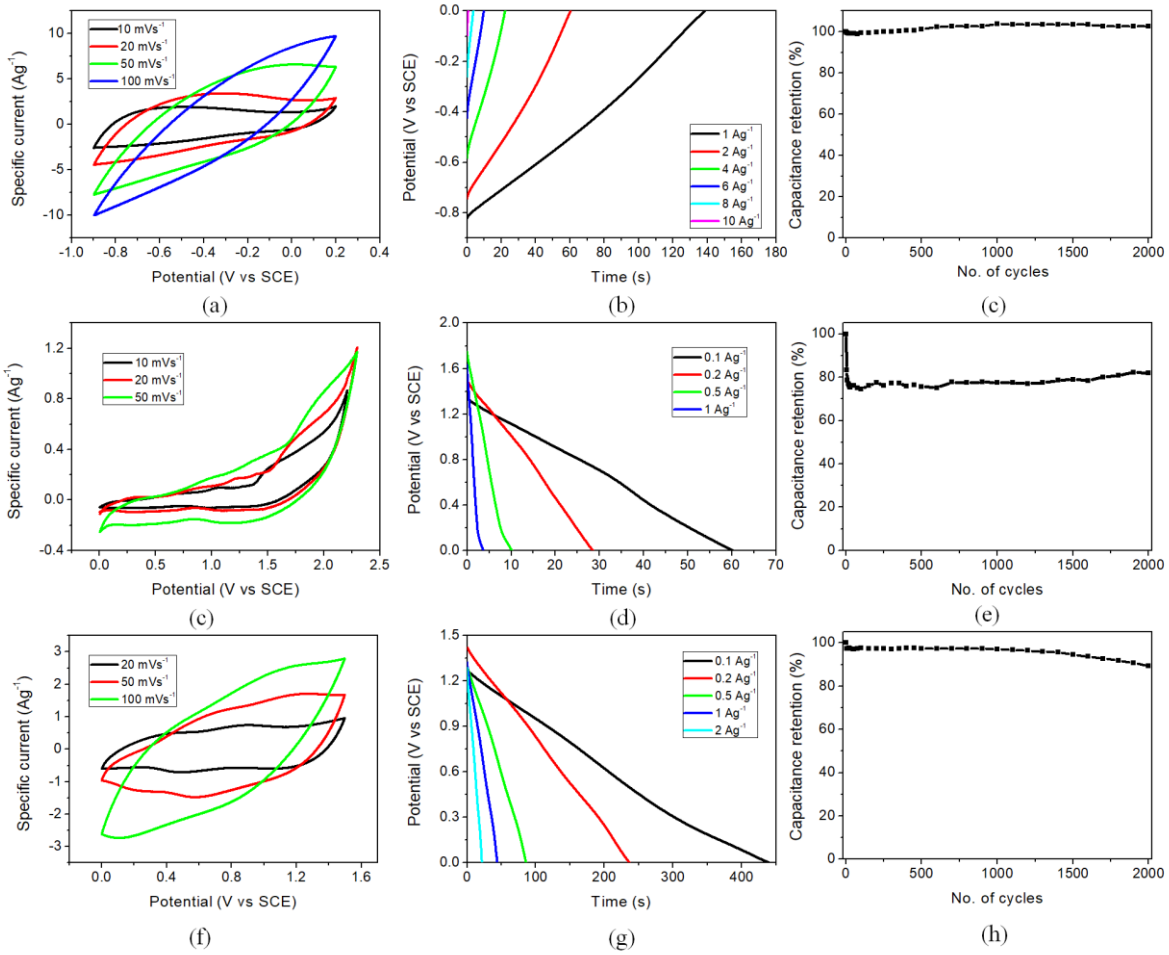

Figure 6 Results of Carbon: voltammograms at different scan rates(a); discharge curves for different current densities (b), cycling stability for 2000 cycles(c); Results of Co nanofoam-C asymmetric cell: Voltammograms at different scan rates (d), discharge curves discharge curves for different current densities (e), cycling stability for 2000 cycles (f); Results of chemically treated Co foam (5%H_2O_2-24h)-C asymmetric cell: Voltammograms at different scan rates (g), discharge curves discharge curves for different current densities (h), cycling stability for 2000 cycles(i)

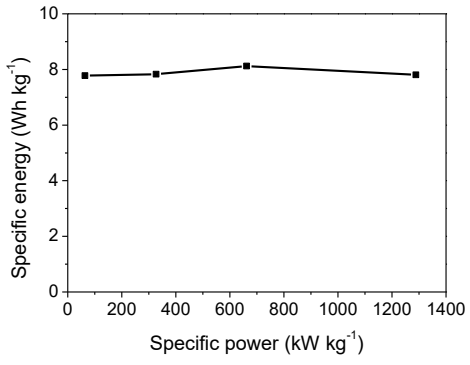

Figure 7 Ragone plot of asymmetric cell with chemically treated Co nanofoam (5% H_2O_2-24h)-Carbon

CONCLUSIONS

The electrochemical performance of the Co nanofoam exhibited a combination of pseudocapacitive and intercalation partial redox response. Thermal treatment at lower temperature than 250^0C did not show any remarkable differences in the electrochemical performance while at higher temperature, the performance became more intercalation controlled due to the presence of Co_3O_4. Co nanofoam, chemically treated with 5% H_2O_2 for 24 hours, showed a significant increase of about 360% in the specific capacity at $1Ag^{-1}$ from 5.7 mAh g^{-1} to 26.1 mAh g^{-1}. Asymmetric cell fabricated with chemically treated Co nanofoam (5% H_2O_2 - 24h) as the positive and carbon as the negative electrode exhibited pseudocapacitive response with excellent rate stability. Only 2% decrease in specific capacitance from 34.6 Fg^{-1} to 33.9 Fg^{-1} was observed with twenty-fold increase in current from 0.1 Ag^{-1} to 2 Ag^{-1}. The cell exhibited specific energy of 7.8 Wh kg^{-1} for specific power of 63.6 kW kg^{-1} which did not show any meaningful change at 1288 kW kg^{-1}. The asymmetric cell showed 90% capacitance retention after 2000 cycles of charge discharge. To conclude, chemically treated Co nanofoam with 5% H_2O_2 for 24 hours shows

remarkable potential as positive electrode material with excellent rate stability in asymmetric cell.

ACKNOWLEDGEMENT

The author thanks Politécnico de Lisboa for receiving scientific initiation fellowship for this work under “IDI&CA/SuperStore 0712045/ISEL” project.

REFERENCE

1. González, A., Goikolea, E., Barrena, J. A. & Mysyk, R. Review on supercapacitors: Technologies and materials. *Renew. Sustain. Energy Rev.* **58**, 1189–1206 (2016).
2. Chen, G. Z. Supercapacitor and supercapattery as emerging electrochemical energy stores. *Int. Mater. Rev.* **62**, 173–202 (2017).
3. SIMON, P. & GOGOTSI, Y. Materials for electrochemical capacitors. in *Nanoscience and Technology* 320–329 (Co-Published with Macmillan Publishers Ltd, UK, 2009). doi:10.1142/9789814287005_0033
4. Wang, G., Zhang, L. & Zhang, J. A review of electrode materials for electrochemical supercapacitors. *Chem. Soc. Rev.* **41**, 797–828 (2012).
5. Zhan, Y. *et al*. Bestow metal foams with nanostructured surfaces via a convenient electrochemical method for improved device performance. *Nano Res.* **9**, 2364–2371 (2016).
6. Popov, K. I., Djokić, S. S., Nikolicć, N. D. & Jović, V. D. *Morphology of electrochemically and chemically deposited metals*. *Morphology of Electrochemically and Chemically Deposited Metals* (2016). doi:10.1007/978-3-319-26073-0
7. Siwek, K. I., Eugénio, S., Silva, T. M. & Fatima Montemor, M. Electrodeposited Manganese Oxide on Tailored 3D Bimetallic Nanofoams for Energy Storage Applications. *Energy Technol.* **7**, 1801139 (2019).
8. Gogotsi, Y. & Penner, R. M. Energy Storage in Nanomaterials – Capacitive, Pseudocapacitive, or Battery-like? *ACS Nano* (2018). doi:10.1021/acsnano.8b01914
9. Upadhyay, K. K., Nguyen, T., Silva, T. M., Carmezim, M. J. & Montemor, M. F. Pseudocapacitive response of hydrothermally grown MoS 2 crumpled nanosheet on carbon fiber. *Mater. Chem. Phys.* (2018). doi:10.1016/j.matchemphys.2018.06.029
10. Subramani, K., Kowsik, S. & Sathish, M. Facile and Scalable Ultra-fine Cobalt Oxide/Reduced Graphene Oxide Nanocomposites for High Energy Asymmetric Supercapacitors†. *ChemistrySelect* **1**, 3455–3467 (2016).